Tight-binding interatomic potentials based on total-energy calculation: Application to noble metals using molecular-dynamics simulation

G. C. Kallinteris, N. I. Papanicolaou, and G. A. Evangelakis
Department of Physics, Solid State Division, University of Ioannina, P.O. Box 1186, GR-45110 Ioannina, Greece

D. A. Papaconstantopoulos
Complex Systems Theory Branch, Naval Research Laboratory, Washington, D.C. 20375-5345

(Received 26 June 1996)

We present an alternate approach to parametrizing the expression for the total energy of solids within the second-moment approximation (SMA) of the tight-binding theory. In order to obtain the necessary parameters, we do not use the experimental values of the lattice constant, the elastic constants, and the cohesive energy, but we fit to the total energy obtained from first-principles augmented-plane-wave calculations as a function of volume. In addition, we shift the total-energy graphs uniformly so that at the minimum they give the experimental value of the cohesive energy. We have applied the above methodology to perform molecular-dynamics simulations of the noble metals. For Cu and Ag our results for vacancy formation energies, relaxed surface energies, phonon spectra, and various temperature-dependent quantities are of comparable accuracy to those found by the standard SMA, which is based on fitting to several measured data. However, our approach does not seem to work as well for Au. [S0163-1829(97)00903-X]

I. INTRODUCTION

In the last 15 years atomistic simulations have played an increasingly important role in many areas of condensed-matter and materials science.[1–3] Crucial to the success of any simulation is the interatomic potential. One of the approaches is the first-principles molecular dynamics (MD) introduced by Car and Parrinello;[4] this scheme provides an accurate description of atomic interactions, but requires enormous computational time, so it is restricted to short simulation times and to a few hundred atoms. Another one deals with empirical potentials, which in many cases reproduce very fast and with satisfactory accuracy the thermodynamic and structural properties of materials. Some of these methods in metallic systems are the embedded-atom method,[5] the effective-medium theory,[6] the Finnis-Sinclair potentials,[7] and the second-moment approximation (SMA) to the tight-binding (TB) model.[8] Recently, a scheme has been proposed, which is between the above two approaches, the so-called tight-binding molecular dynamics.[9] This method is about two or three orders of magnitude faster than *ab initio* formulations, and at the same time describes with suitable accuracy the electronic structure of the system. Nevertheless, its computational cost remains much higher compared to empirical potentials. Another TB methodology is now advocated by the NRL group.[10–12] This approach has been successful in accurately determining structural energy differences, elastic constants, vacancy formation energies, surface energies and phonon spectra for 29 elements. However, in its present form, this method is too slow for MD simulations.

The TB-SMA method takes into account the essential band character of the metallic bond: the total energy of the system consists of a band-structure term, proportional to the effective width of the electronic band (and so to the square root of the second moment of the local density of states) (Ref. 13) and a repulsive pair-potential term, which incorporates the non-band-structure parts of the total energy, including electrostatic interactions. The expression for the total energy contains a small set of adjustable parameters, which have typically been determined by matching to experimental data of cohesive energy, lattice constant, bulk modulus, and elastic constants of the system.[14,15] It has been found that the quality of the results is improved by including a sufficient number of interacting atoms (typically up to fifth neighbors).[15–17]

The aim of the present work is to use the TB-SMA model, with parameters determined from first-principles calculations rather than from experimental quantities. Our approach consists in adjusting the total-energy expression of the TB-SMA method to augmented-plane-wave (APW) total-energy results. We applied this method to the noble metals, and we tested the quality of our parameters by deriving the bulk modulus, elastic constants, vacancy formation energies, and surface energies of each metal. In addition, we performed MD simulations at various temperatures, obtaining the temperature dependence of the lattice constant and the atomic mean-square-displacements (MSD), as well as the phonon density of states (DOS) and the phonon-dispersion curves. The simulated quantities are compared with available experimental data. It has to be noted here that this method can be particularly useful, especially in cases where all the necessary experimental values (cohesive energy, elastic constants, etc.) are not known, e.g., stoichiometric alloys, disordered systems, etc., and hence the usual procedure of fitting to experimental data is not feasible.

This article is organized as follows. Section II describes the method of calculation and the various computational details. In Sec. III we discuss numerical results of elastic constants, vacancy formation energies, surface energies, and temperature-dependent quantities obtained from MD simulations, as well as their comparison with experimental values. Summary and conclusions are given in Sec. IV.

II. METHOD OF CALCULATION

The band structure of the noble metals Cu, Ag, and Au was calculated by the symmetrized APW method[18] in the muffin-tin approximation. The self-consistent semirelativistic calculations yielded the crystal potential, the charge density, and the eigenvalue sum, which were used in Janak's expression for the total energy.[19] The exchange and correlation was treated by the Hedin-Lundqvist formalism.[20] The computations were done for both the fcc and bcc structures of metals; we used a mesh of 89 **k** points in the irreducible Brillouin zone for the fcc and 55 **k** points for the bcc structure. The total energy was calculated for five different lattice parameters for each structure and the resulting variation was fitted to a parabolic function.[21] More details of these calculations are given by Sigalas, Papaconstantopoulos, and Bacalis.[22]

In the TB-SMA model,[8,13] the total energy of the system is written as

$$E=\sum_i (E_i^B+E_i^R), \tag{1}$$

where E_i^B represents the band-structure term,

$$E_i^B=-\xi\sqrt{\sum_{j\neq i} e^{-2q[(r_{ij}/r_0)-1]}}, \tag{2}$$

and E_i^R is a pair-potential repulsive term (Born-Mayer type),

$$E_i^R=A\sum_{j\neq i} e^{-p[(r_{ij}/r_0)-1]}. \tag{3}$$

In expressions (2) and (3), r_{ij} is the distance between atoms i and j, and the sums include interactions up to fifth neighbors. r_0 is usually fixed to the value of the first-neighbor distance. In our case r_0 is an additional free parameter, as suggested in Ref. 23. Therefore, there are five parameters ξ, A, q, p, and r_0 in our scheme, which have been determined from Eqs. (1)–(3) for each element by fitting to the APW total-energy results as a function of lattice constant for both the fcc and bcc structures. We used the total energies of each metal for both the fcc and bcc structures, since it was found that the agreement with the experimental values for the elastic constants was better than the one obtained when using only the fcc structure.[23] We note here that, in practice, before performing the fitting procedure, we convert to cohesive energies by subtracting from both the fcc and bcc APW total energies the energy of an isolated atom, as it was calculated in the local-density approximation (LDA) using a relativistic formalism.[24] Since it is well known that the total energy of isolated atoms is poorly described by the LDA, we shifted the computed cohesive energies, so that the absolute minimum of the fcc structure coincides with the experimental cohesive energies. The elastic constants of the metals were calculated at the experimental lattice constant from the difference in total energies of the distorted and undistorted lattices.

Using the above interatomic potential, we performed MD simulations in the microcanonical ensemble in order to validate the model at various temperatures. The system is made up of 4000 particles arranged on a fcc lattice. The simulation box contained 40 atomic layers with 100 atoms each, in which periodic boundary conditions were imposed in the three space directions. The equations of motion were integrated by means of the Verlet algorithm and a time step $\delta t=5\times10^{-15}$ s guarantees a total-energy conservation within $\delta E/E=10^{-5}$. The system was equilibrated at a desired temperature during 1000 integration time steps (5 ps), which

TABLE I. Calculated (Calc.) and experimental (Expt.) lattice constants (Ref. 26), a, along with the cohesive energies (Ref. 27) E_c, for the three noble metals.

Element	a (Å)		E_c (eV)	
	Calc.	Expt.	Calc.	Expt.
Cu	3.53	3.60	4.65	3.54
Ag	4.03	4.07	3.62	2.96
Au	4.06	4.07	3.77	3.78

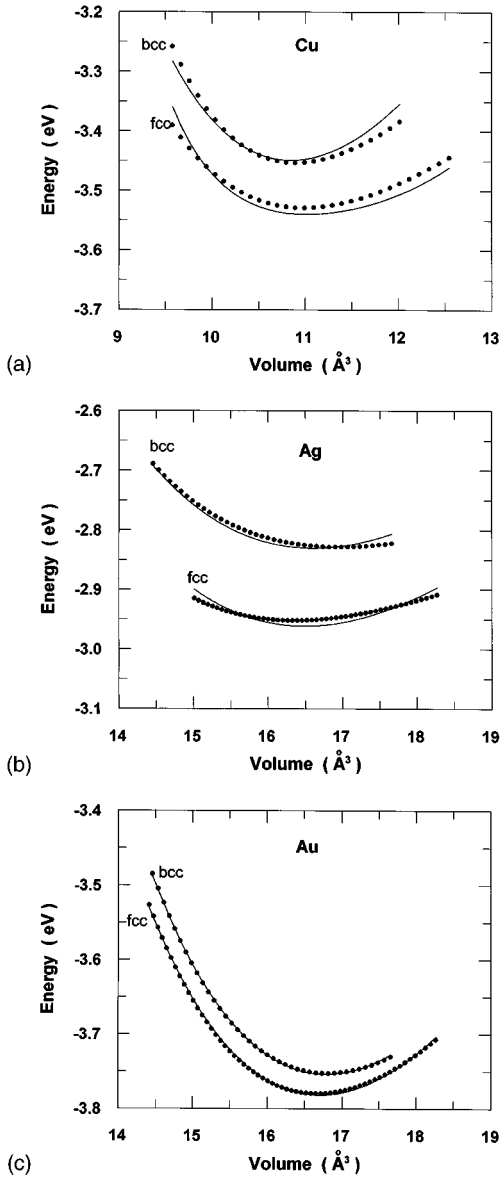

FIG. 1. Calculated cohesive energies (with opposite sign) of (a) Cu, (b) Ag, and (c) Au as a function of volume. Solid lines correspond to the APW results; filled symbols refer to the results of the fit [Eqs. (1)–(3)].

TABLE II. Potential parameters for tight-binding second-moment approximation as obtained by fitting the computed volume dependence fo the cohesive energies to Eqs. (1)–(3).

Element	ξ (eV)	A (eV)	q	p	r_0 (Å)
Cu	1.9840	13.1610	1.0844	9.3582	1.5564
Ag	0.7824	0.5354	0.9248	15.8659	3.4733
Au	10.9249	13.5959	2.7381	6.3469	1.7517

were sufficient to obtain stationary values for the potential and kinetic energies. Another 5000 additional steps (25 ps) were performed to calculate time averages. By performing four times longer trajectories, we did not find significant changes in the computed quantities. The vacancy formation and surface energies were calculated at $T=0$ K by performing a quasidynamic minimization procedure[25] integrated in the MD code. The free surfaces were produced by fixing the dimensions of the computational box at a value twice as large as the thickness of the crystal along the z direction; an infinite slab was thus constructed delimited by two free surfaces parallel to (100), (110), or (111) planes.

The value of the lattice constant at each temperature was chosen so as to result in zero pressure in the system, while the atomic mean-square displacements were determined on a layer-by-layer basis from equilibrium averages of the atomic density profiles. Finally, the phonon DOS was obtained from the Fourier transform of the velocity autocorrelation function, and the phonon spectral densities were calculated by Fourier transforming the velocity- and position-dependent autocorrelation function for a given polarization and a specific **k** vector in the Brillouin zone. Details of this computational procedure can be found elsewhere.[17] Consequently, the phonon-dispersion curves were deduced from frequencies found in the corresponding spectral densities. In particular, we used a mesh of ten **k** vectors along each symmetry direction, and then we performed a cubic spline interpolation.

III. RESULTS AND DISCUSSION

In Table I we present results for the calculated equilibrium lattice constants[22] and cohesive energies[24] of the three materials under study, along with the corresponding experimental values.[26,27] The predicted lattice constants are consistent with the known effects of the scalar relativistic LDA: for Cu, a $3d$ element, the error (compared to experiment[26]) is 1.9%, while for Ag, a $4d$ element, the calculated lattice parameter is 0.7% smaller than the measured value.[26] The agreement is much better for Au, a $5d$ metal, where there is a remarkable accuracy. On the other hand, the cohesive energies of Cu and Ag are overestimated by 31% and 22%, respectively, a result reflecting the well-known deficiency of the LDA for atoms, while for Au, surprisingly, the agreement is very good.

TABLE III. Bulk modulus B and elastic constants (in GPa) for the noble metals computed in the TB-SMA method. The calculations were performed at the experimental lattice constants, and the measured elastic constants are taken from Ref. 26.

Element	Calculated (GPa)				Experimental (GPa)			
	B	C_{11}	C_{12}	C_{44}	B	C_{11}	C_{12}	C_{44}
Cu	118	155	99	85	137	168	121	75
Ag	82	109	68	53	103	124	93	46
Au	169	184	161	28	169	189	159	42

TABLE IV. Tight-binding second-moment approximation vacancy formation energies along with the experimental values (Ref. 28) for the materials under study.

Element	Vacancy formation energy (eV)	
	Present work	Experiment
Cu	1.50	1.28–1.42
Ag	1.33	1.11–1.31
Au	0.49	0.89±0.04

In Figs. 1(a)–(c) we show the opposite of the computed cohesive energies of noble metals as a function of the volume in the fcc and bcc structures (solid lines) after the appropriate energy shift, as discussed in Sec. II. In the same figure we also present the results of the fit (filled symbols) as computed by Eqs. (1)–(3). We note that the maximum difference between the TB-SMA fitted energies and the first-principles energies for Cu and Ag is about 0.02 eV, and even smaller for the case of Au.

The potential parameters of the TB-SMA scheme, are given in Table II for the three materials under study. We remind the reader that r_0 is taken as a free parameter, and thus it has nothing to do with the first-neighbor distance, the value that is usually used, and which is kept fixed at the experimental value of the fcc structure in other works.[14–17]

In Table III we report the computed bulk modulus and elastic constants of noble metals, along with the corresponding measured values.[26] The calculations were performed in the TB-SMA scheme using the experimental lattice constants at room temperature. The accuracy of the elastic constants, showing a deviation of 10–20 % from experiment is comparable to that of first-principles calculations, and to the TB method of Ref. 12.

We also determined the vacancy formation energies, using the quasidynamic minimization method integrated in the

TABLE V. Surface energies of noble metals, obtained from our molecular-dynamics simulations, along with the experimental values (Refs. 29 and 30).

Element	Surface	Surface energy (J/m^2) Calculated	Experimental
Cu	(100)	1.76	
	(110)	1.89	1.77
	(111)	1.68	
Ag	(100)	1.39	
	(110)	1.47	1.25–1.32
	(111)	1.38	
Au	(100)	0.44	
	(110)	0.45	1.50–1.54
	(111)	0.37	

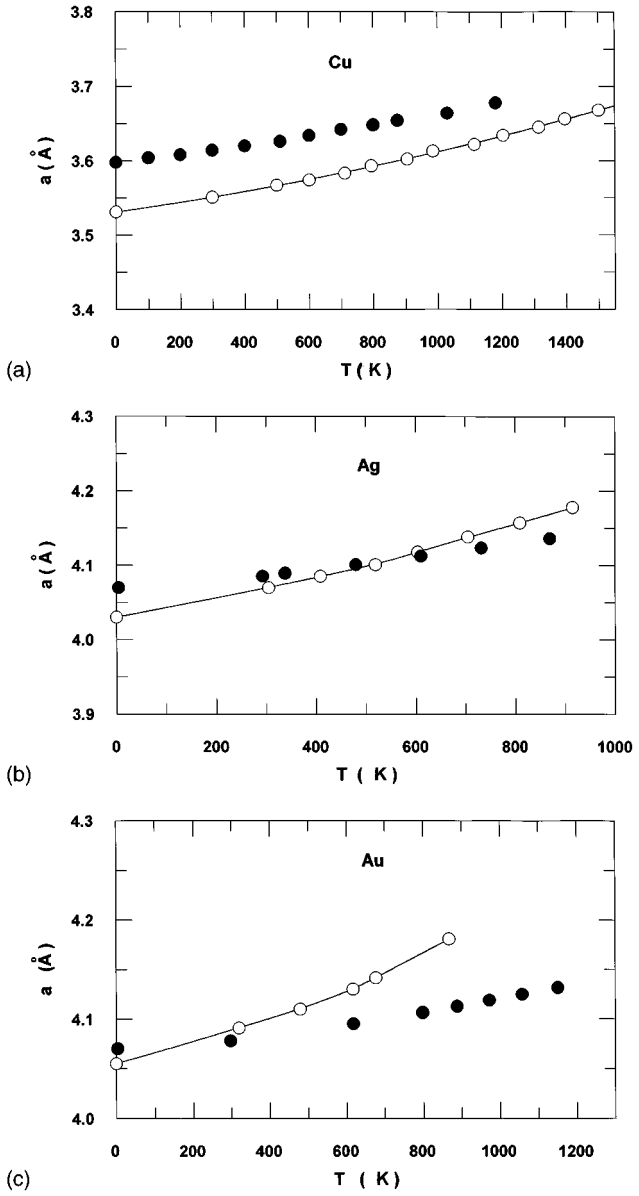

FIG. 2. Temperature dependence of lattice constants of (a) Cu, (b) Ag, and (c) Au. The open and filled circles correspond, respectively, to the results of the simulation and the experiment. The experimental data for Cu are taken from Ref. 31, and for Ag and Au from Ref. 32.

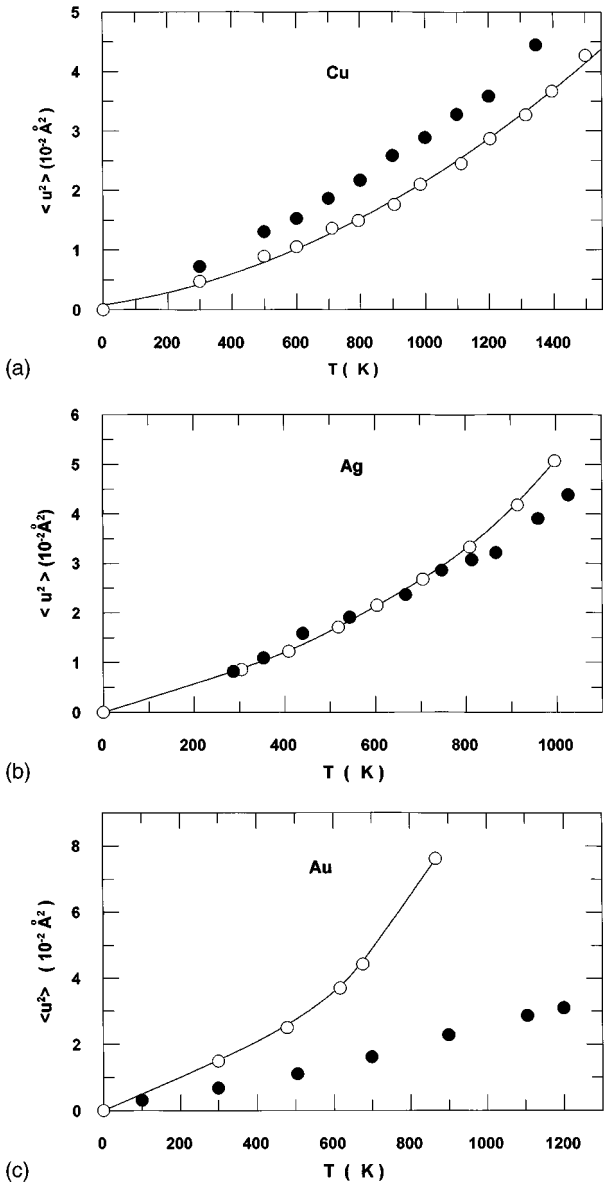

FIG. 3. Mean-square displacements of (a) Cu, (b) Ag, and (c) Au as a function of temperature. The open circles and the lines correspond to the results of our simulation, while the filled circles are the experimental data from Refs. 34, 35, and 36 for Cu, Ag, and Au, respectively.

MD code and the procedure described in Sec. II. Results for this quantity, after relaxation of the whole system, are summarized in Table IV together with the available experimental values.[28] We see that the TB-SMA method predicts vacancy formation energies for Cu and Ag, which are close to experiment, but for Au this energy is much lower than the experimental value. Furthermore, our values compare well with those of another TB-SMA simulation,[15] where the necessary parameters have been obtained by fitting to experimental quantities. It is interesting to note that the elaborate TB method of Ref. 12 gives a better value of the formation energy of Au.

We have also calculated the relaxed surface energies of low index faces (100), (110), and (111) for the noble metals. Table V compares these results to experiment.[29,30] We note that the experimental energies refer to polycrystalline surfaces. Our MD simulations follow the trends usually observed on fcc metal surfaces: the smallest surface energy is that of the (111) face, while the largest one is that of the (110) face. These results are compatible with the fact that close-packed surfaces are the most stable for the fcc metals. The surface energies for Cu and Ag are very close to experiment, while for Au the predicted values are smaller than the experimental value by a factor of 3.

In the following we present some finite-temperature properties. In Figs. 2(a)–2(c) we show the lattice constants of noble metals as a function of temperature, as deduced from our MD simulations, along with the corresponding experimental values.[31,32] It is clear, from this figure, that the best agreement with the measured values is achieved for Ag [Fig. 2(b)], while for Cu there is a deviation of 1.9% between the computed and the experimental values at low temperature,

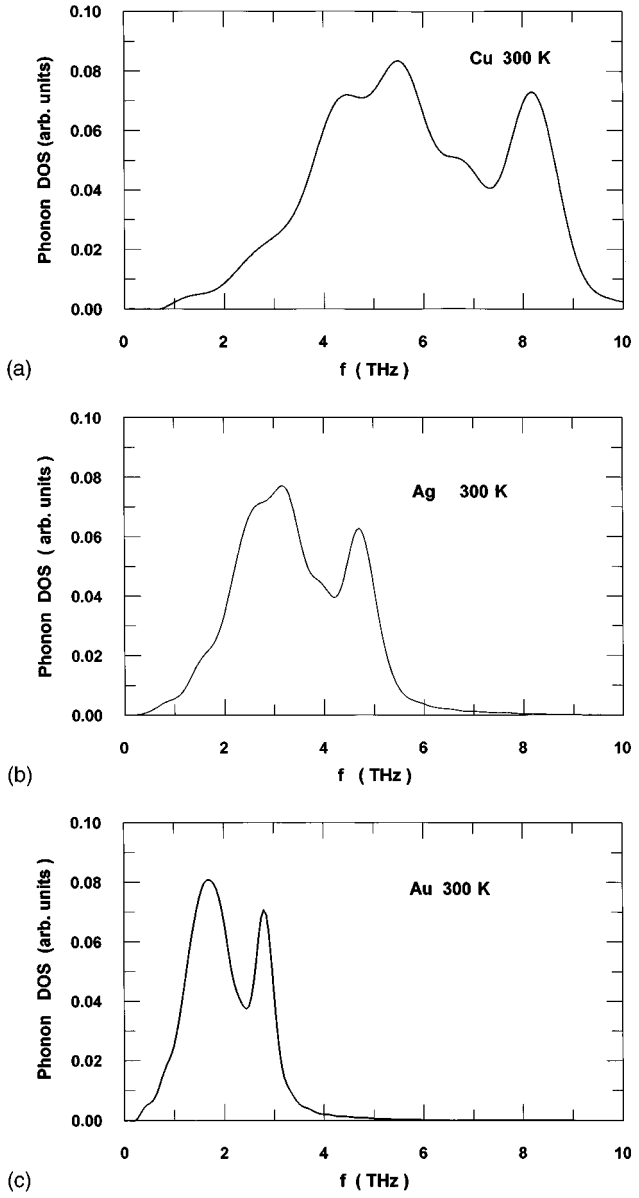

FIG. 4. Phonon DOS of (a) Cu, (b) Ag, and (c) Au at 300 K derived from our MD simulation.

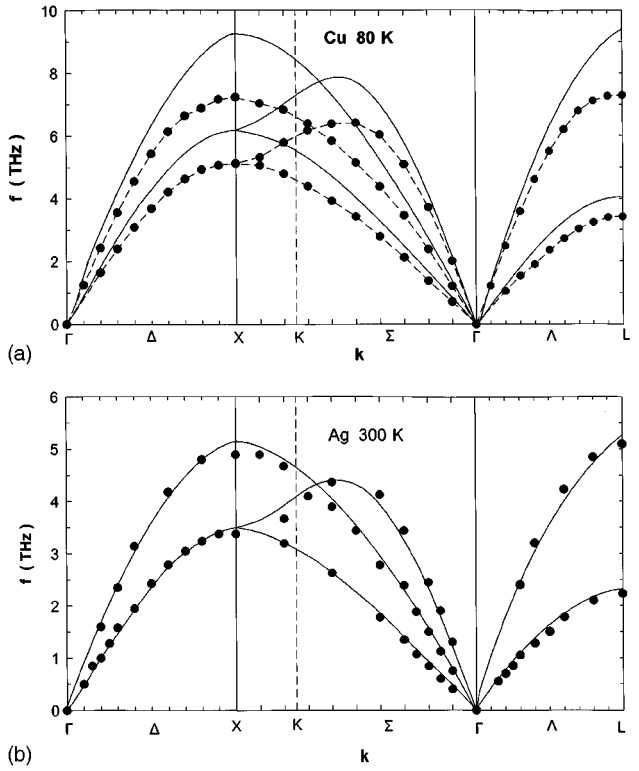

FIG. 5. Phonon-dispersion curves for (a) Cu at 80 K and (b) Ag at 300 K along the high-symmetry directions. Solid lines correspond to MD results after a cubic spline interpolation; filled circles refer to the experimental data from Ref. 41 for Cu and Ref. 39 for Ag.

which becomes smaller with increasing temperature [Fig. 2(a)]. It is worth noting that the resulting thermal-expansion coefficients are in good agreement with the experiment for both metals. In the case of Au, despite the accuracy obtained at low temperatures, the discrepancy increases progressively at high temperatures, where the simulation predicts larger lattice dilation from the measurement [Fig. 2(c)]. A similar behavior has been also found in a Monte Carlo study[33] using a TB-SMA potential model, where the parameters were adjusted to the experimental data.

In Figs. 3(a)–3(c) we compare the temperature dependence of our computed atomic MSD's (solid curves) with experimental data for Cu,[34] Ag,[35] and Au.[36] Our values are slightly underestimated for Cu [Fig. 3(a)], a fact which is consistent with the lower values of the lattice constant at various temperatures by our TB-SMA potential. The agreement for Ag is again very good [Fig. 3(b)], denoting the success of the proposed scheme for this element. Concerning Au, the disagreement is evident [Fig. 3(c)]; for example, the MSD's at 700 K are more than twice as large as the experimental value, a fact which has been also found in the TB-SMA Monte Carlo study.[33] According to Lindemann's criterion,[37] the melting point can be empirically estimated by the MSD values; therefore, it is clear that the present model results in an anticipated melting of the gold. A similar underestimation of the melting point has been also found by Cleri and Rosato,[38] although they have fitted the free parameters of their TB-SMA scheme to the experimental values of cohesive energy, lattice constant, and elastic constants for Au. We can thus conclude that this discrepancy for Au is not due to the quality of our TB-SMA parameters, but it is probably related to the second moment approximation.

Following Lindemann's criterion, we deduce the approximative melting temperatures of Cu, Ag, and Au to be 1450 ± 50, 1100 ± 50, and 850 ± 50 K, respectively, to be compared to the experimental values of 1358, 1235, and 1338 K.[27]

The phonon DOS's for the elements under study are presented in Figs. 4(a)–4(c) at room temperature. We see that the main features of the phonon frequency spectra are well reproduced; we note that, since in our calculations we use the Fourier transform of the velocity autocorrelation function, the DOS shape is smoothed. Comparing our phonon DOS of Cu [Fig. 4(a)] with previous works based on TB-SMA potentials,[15,16] resulting from fitting to experimental quantities, we observe a reasonable agreement, except of a slight shift toward higher frequencies, present in our spectrum. In

the case of Ag [Fig. 4(b)] the cutoff frequency is well predicted by our simulations, in agreement with a previous computation[15] and measurements.[39] For Au [Fig. 4(c)] the same quantity is considerably underestimated (we find about 3.25 THz compared to 4.7 THz, which is the experimental value), a result also found in Ref. 15. The phonon DOS of Au is thus too narrow, compared to the experiment.[40] This is consistent with the previous remarks about large lattice dilation at high temperature, excessive MSD's, and anticipated melting of the system. The failure of the model for Au can be attributed to the contribution of noncentral many-body forces, not included in the second-moment approximation.[15] One could overcome this discrepancy by taking into account higher-order moments. Furthermore, in a recent work using the tight-binding total-energy method,[10] without the limitations of the SMA, the phonon frequency spectrum of Au is better reproduced than in the present study.

The phonon-dispersion curves of Cu (80 K) and Ag (300 K) are displayed in Figs. 5(a) and 5(b), respectively, together with the experimental results.[41,39] The agreement between simulation and measurements is excellent for Ag, while for Cu the main features are reproduced, but there is an overestimation of the cutoff frequency in the vicinity of the Brillouin-zone boundaries.

IV. CONCLUSIONS

We presented a modified method of determining the parameters of tight-binding second-moment approximation interatomic potentials by adjusting the corresponding expressions to first-principles total-energy calculations. The resulting scheme was applied to the noble metals and we obtained the bulk modulus, elastic constants, vacancy formation, and surface energies for each metal. We found a good agreement with the experiment, except for the vacancy formation energy and surface energy of gold, which were considerably underestimated. Furthermore, we performed finite-temperature molecular-dynamics simulations to determine the temperature dependence of the lattice constants and atomic mean-square displacements, as well as the phonon density of states and phonon-dispersion curves. The predicted values compare very well with the experimental data for silver, while they are in acceptable agreement for copper. It should be mentioned that, despite the fact that we did not use the experimental data to determine the necessary TB-SMA parameters, we obtained a comparable accuracy to that found by the standard SMA, in which the parameters are adjusted to the experimental quantities. Concerning gold, the model fails to reproduce its high-temperature properties. It should be noted that this is not due to the quality of our TB-SMA parameters, but to the failure of second-moment approximation. Including higher-order moments, the agreement with experiment could be improved. The procedure described here can be extended to binary stoichiometric or even disordered systems, especially in cases where there are not enough available experimental data to obtain the TB-SMA parameters.

ACKNOWLEDGMENTS

This work was partially supported by ΠΕΝΕΔ Grant No. 1654/1995 of the Greek Ministry of Development and NATO Grant No. CRG-940118. We thank Dr. M. Mehl for discussions and for providing calculated atomic energies.

[1] *Computer Simulation in Materials Science*, edited by M. Meyer and V. Pontikis (Kluwer, Dordrecht, 1991).
[2] *Computer Simulation in Chemical Physics*, edited by M. P. Allen and D. J. Tildesley (Kluwer, Dordrecht, 1993).
[3] *Computer Simulation in Materials Science*, edited by H. O. Kirchner, L. P. Kubin, and V. Pontikis (Kluwer, Dordrecht, 1996).
[4] R. Car and M. Parrinello, Phys. Rev. Lett. **55**, 2471 (1985).
[5] M. S. Daw and M. I. Baskes, Phys. Rev. B **29**, 6443 (1984); S. M. Foiles, M. I. Baskes, and M. S. Daw, *ibid*. **33**, 7983 (1986).
[6] J. K. Nørskov, Rep. Prog. Phys. **53**, 1253 (1990).
[7] M. W. Finnis and J. E. Sinclair, Philos. Mag. A **50**, 45 (1984).
[8] F. Ducastelle, J. Phys. (Paris) **31**, 1055 (1970).
[9] A. P. Sutton, P. D. Godwin, and A. P. Horsfield, MRS Bull. No.2, 42 (1996), and references therein.
[10] R. E. Cohen, M. J. Mehl, and D. A. Papaconstantopoulos, Phys. Rev. B **50**, 14 694 (1994).
[11] M. J. Mehl and D. A. Papaconstantopoulos, Europhys. Lett. **31**, 537 (1995).
[12] M. J. Mehl and D. A. Papaconstantopoulos, Phys. Rev. B **54**, 4519 (1996).
[13] D. Tomanek, A. A. Aligia, and C. A. Balseiro, Phys. Rev. B **32**, 5051 (1985); W. Zhong, Y. S. Li, and D. Tomanek, *ibid*. **44**, 13 053 (1991).
[14] V. Rosato, M. Guillope, and B. Legrand, Philos. Mag. A **59**, 321 (1989).
[15] F. Cleri and V. Rosato, Phys. Rev. B **48**, 22 (1993).
[16] B. Loisel, D. Gorse, V. Pontikis, and J. Lapujoulade, Surf. Sci. **221**, 365 (1989); B. Loisel, J. Lapujoulade, and V. Pontikis, *ibid*. **256**, 242 (1991).
[17] N. I. Papanicolaou, I. E. Lagaris, and G. A. Evangelakis, Surf. Sci. **337**, L819 (1995).
[18] L. F. Mattheiss, J. H. Wood, and A. C. Switendick, Methods Comput. Phys. **8**, 63 (1968).
[19] J. F. Janak, Phys. Rev. B **9**, 3985 (1974).
[20] L. Hedin and B. I. Lundqvist, J. Phys. C **4**, 2064 (1971).
[21] F. Birch, J. Geophys. Res. **83**, 1257 (1978).
[22] M. Sigalas, D. A. Papaconstantopoulos, and N. C. Bacalis, Phys. Rev. B **45**, 5777 (1992).
[23] M. M. Sigalas and D. A. Papaconstantopoulos, Phys. Rev. B **49**, 1574 (1994).
[24] M. J. Mehl (private communication).
[25] C. H. Bennett, in *Diffusion in Solids, Recent Developments*, edited by A. S. Nowick and J. J. Burton (Academic, New York, 1975), p. 73.
[26] G. Simmons and H. Wang, *Single Crystal Elastic Constants and Calculated Aggregate Properties: A Handbook*, 2nd Ed. (MIT Press, Cambridge, MA, 1971).
[27] C. Kittel, *Introduction to Solid State Physics*, 3rd ed. (Wiley, New York, 1966).
[28] H.-E. Schaefer, Phys. Status Solidi A **102**, 47 (1987).

[29] W. R. Tyson and W. A. Miller, Surf. Sci. **62**, 267 (1977).
[30] F. R. De Boer, R. Boom, W. C. M. Mattens, A. R. Miedema, and A. K. Niessen, *Cohesion in Metals* (North-Holland, Amsterdam, 1988).
[31] P. C. Gehlen, Phys. Rev. **129**, 715 (1963).
[32] W. B. Pearson, *A Handbook of Lattice Spacings and Structures of Metals and Alloys* (Pergamon, Oxford, 1967).
[33] H. M. Polatoglou and G. L. Bleris, Interf. Sci. **2**, 31 (1994).
[34] C. J. Martin and D. A. O'Connor, J. Phys. C **10**, 3521 (1977).
[35] M. Simerska, Acta Crystallogr. **14**, 1259 (1961); C. W. Haworth, Philos. Mag. **5**, 1229 (1960).
[36] E. A. Owen and R. W. Williams, Proc. R. Soc. London, Ser. A **188**, 509 (1947).
[37] F. A. Lindemann, Phys. Z. **11**, 609 (1910).
[38] F. Cleri and V. Rosato, Philos. Mag. Lett. **67**, 369 (1993).
[39] W. A. Kamitakahara and B. N. Brockhouse, Phys. Lett. **29A**, 639 (1969).
[40] J. W. Lynn, H. G. Smith, and R. M. Nicklow, Phys. Rev. B **8**, 3493 (1973).
[41] G. Nilsson and S. Rolandson, Phys. Rev. B **7**, 2393 (1973).